Indian Journal of Geo Marine Sciences
Vol. 48 (07), July 2019, pp. 1091-1097

Experimental study on hydrodynamic characteristics of underwater glider

Muhammad Yasar Javaid[1,2*], Mark Ovinis[1], Maria Javaid[3], & Barkat Ullah[1,4]

[1]Department of Mechanical Engineering, Universiti Teknologi PETRONAS, Perak, Malaysia
[2]Department of Mechanical Engineering Technology, Government College University Faisalabad, Pakistan
[3]Department of Mathematics, Government College University Faisalabad, Pakistan
[4]Department of Electrical Engineering. COMSATS University Islamabad Abbottabad campus
*[E-Mail: yasarjavaid@gcuf.edu.pk]

The enhancement of the hydrodynamic characteristics of autonomous underwater gliders (AUGs) is an important factor because of their weak inner propulsion system and altitude control. Moreover, resistance forces acting on the glider limit its operational range and increase energy utilisation. In this paper, towing tanks experiments were conducted to investigate the hydrodynamic characteristic of a newly developed underwater glider with fixed wings and a tail rudder. Specifically, this work presents the hydrodynamic performance of a newly developed AUG in a horizontal plane towed tank environment. This hydrodynamic study investigates the glider performance at a wide range of speed (0.3-0.7 m/sec) and drift angles (0-18^0). The resistance forces were measured by internal strain gauges, mounted on the towing carriage. The experimental results were used to analyse the resistance with variation in Froude's number and drift angles, using Reynold's Average Navier Stoke equation in Ansys FLUENT. Both experimental and simulation are well corroborated and show that resistance force is a strong function of the drift angle. The results are useful for the potential development of AUGs and their control surfaces.

[**Keywords:** Autonomous underwater glider; Towing tank; Hydrodynamic characteristic; CFD simulation]

Introduction

Autonomous underwater gliders (AUGs) play a vital role in exploring the hidden resources of oceans, continuous environment monitoring, and deep-sea oil and gas exploration[1]. Recent developments in glider design have seen their rapid application in a variety of deepwater applications. These important design aspects are centred towards improving payload capacity, increasing volume and enhancing wing shape.

Stevenson et al.[2] studied the impact of hull shape and size on the hydrodynamic forces and moments of gliders. They found that the speed and operational range of a glider is a function of resistance or drag force. Most of the glider energy is consumed to overcome the drag or resistance forces. The kinetic energy of glider is a function of retarding force (drag) and operational range, given by the equation,

$$D \times R = \frac{1}{2} m v^2 \quad \ldots (1)$$

where, 'D' is the drag force, 'R' is the range of the glider and 'm' is the total glider mass. The lift force 'L' is equal to the total weight of the glider as shown in the equations,

$$L = W = mg \quad \ldots (2)$$

$$R = \frac{L}{D} \frac{v^2}{2g} \quad \ldots (3)$$

AUGs typically comprise a cylindrical hull and fixed wings. Their payload capacity and functionalities are comparable i.e. Slocum [3], Spray [4] and Seaglider [5].

A glider behaves like an aircraft as it is independent of free surface effect unlike surface vessel. Free surface water effect can be ignored because the glider is submerged in water and therefore does not experience any surface effect. However, the submerged vehicles have viscous pressure and frictional resistance. The frictional and viscous (form) resistance is related to the lift-to-drag (L/D) ratio variation, as shown in Figure 1.

The effect of L/D ratio is paradoxical, where the minimum total resistance shows the optimum L/D ratio. The other important fluid characteristics include Reynolds number, given as

$$R_e = \frac{\rho v L}{\mu} \quad \ldots (4)$$

where ρ is the density of water, 'L' is the length of glider, 'v' is the velocity of fluid and 'μ' is the viscosity of fluid. Another important fluid property is

the Froude number (Fr), a dimensionless number which marks the influence of gravity on the fluid motion and indicates how well a model works in a real system.

$$\text{Froude number: } F_r = \frac{v}{\sqrt{gh/D}} \quad \ldots (5)$$

where 'h' is the distance from the undisturbed free surface level of water. Figure 2 shows that the resistance force of submerged body decreases with the increasing submerged depths.

Various researchers have defined a variety of submerged conditions, like Bertram[7] has recommended 5D (h=5D) and Jackson[8] 3D (h=3D).

Mathematical background

The total energy dissipation of a glider hull is related to resistance because of resistance forces. In general, the flow of fluid acts in two ways along the body of glider, first along the body (due to shear stress, τ) and the second is normal direction force to the glider (due to surrounding pressure, p). The force opposite of flow direction is called resistance (drag) force and normal force component of flow is the lift force of the glider. The total resistance on the glider is split into friction, form and wave resistance[9]. Figure 3 shows the total resistance of submerged vehicles, modified from surface vehicles.

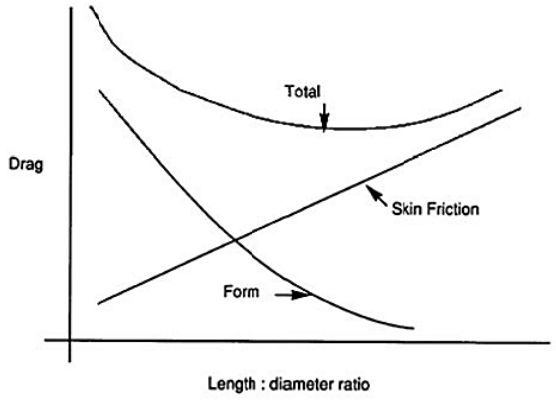

Fig. 1 — Variation of glider resistance with L/D ratio [6]

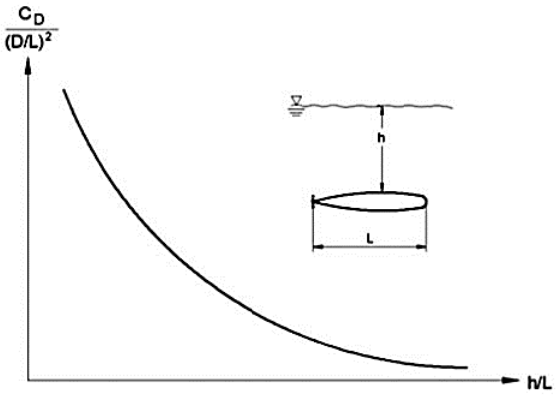

Fig. 2 — Total resistance with depth variation[6]

Waves occur due to changing water pressure near the free surface interface between air and water. When a glider moves away from the surface to submerged condition, the effect of waves decreases until it is completely absent; skin friction resistance is due to the viscosity of fluid.

Drag or resistance force at the boundary layer along the length of hull is due to forces moving fluid around the body. The hull is assumed to be a smooth rigid body fully submerged in incompressible fluid flow.

Flow across the body is grouped into three regions as shown in Figure 4. The boundary layers near the body constitute viscous flow. The area away from the boundary layers is known as non-viscous or potential flow.

The velocity gradient between the glider hull and the outer flow region exists in the form of a boundary layer[10]. The frictional resistance is estimated through the drag force produced on the body. This is attributed to the turbulent flow over the wetted body surfaces over the total length of the glider hull. The total resistance is equal to pressure resistance R_p and frictional resistance R_F, $R_P = R_T - R_F$.

$$R_T = 0.5 C_T S \rho V^2 \quad \ldots (6)$$

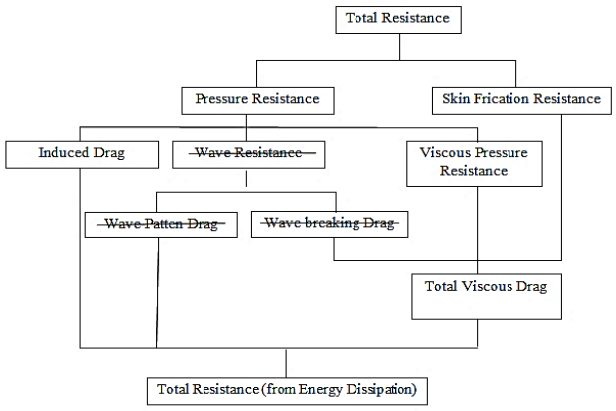

Fig. 3 — Components of total resistance for submerged vehicles[9]

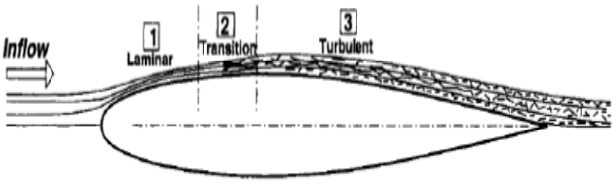

Fig. 4 — Flow pattern around a deeply immersed hull[10]

where 'S' is the wetted surface in still water, V indicates the model speed and ρ the density of the medium i.e. towing tank water. Using the results of the dynamometer in the towing tank, the total drag R_T can be obtained, as given by equation (7).

$$C_T = \frac{R_T}{0.5\rho S V^2} \quad \ldots (7)$$

where C_T is the non-dimensional total resistance (drag) coefficient.

The skin frictional coefficient of the viscous drag force for the design of surface vehicles is a function of Reynolds number recommended in ITTC[11]. The friction drag coefficient is

$$C_F = \frac{0.075}{(\log R_e - 2)^2} \quad \ldots (8)$$

where C_F is the non-dimensional friction drag coefficient and *Re* is the Reynolds number as defined in equation (4).

Simulation Design and Analysis Methods

Experimental Study

The newly developed AUG was tested at the towing tank in Marine Technology Centre (MTC) of Universiti Teknologi Malaysia. The total water channel length was $120 \times 4 \times 2.5$ m^3, filled with fresh water. The towing carriage has variable speed with a dynamometer to measure the forces acting on the model as shown in Figure 5.

Glider model

The glider model was fixed to carriage with struts as shown in Figure 6. The dimensions of the glider are given in Table 1. The struts were passed through the top of the glider to maintain the distance from free surface 3d (d=diameter). An aerofoil shield was used to counter the inherent resistance of the solid struts. The movement of plate and struts relative to the carriage was determined with the help of orthogonally-mounted linear variable differential transformers (LVDTs) and electromechanical transducers. These LVDTs were calibrated before each experiment at high accuracy based on the theoretical estimation of drag force.

Test conditions and set-up

Figure 7 shows the body-fixed coordinates of the glider model. The surge and sway forces are defined horizontally in the x-axis and y-axis of the glider, respectively; and heave is defined in the vertically downward direction along the gravity force of glider in the z-axis.

Table 1 — UTP gliders dimension[12]

Dimension	Taper wings glider
Total wing span (b)	0.97
Root chord length C_r	0.17m
Glider diameter d	0.28m
Taper ratio C_r / C_t	1.89
Sweep angle (a)	8.5^0

Fig. 5 — Towing tank Carriage UTM

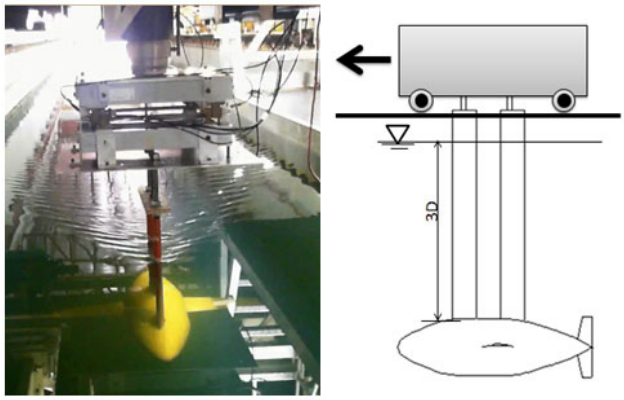

Fig. 6 — Experimental (left) and schematic (right) of model set-up with carriage

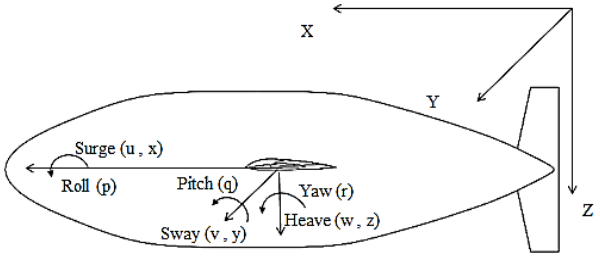

Fig. 7 — Body-fixed coordinate systems of the underwater glider

In the towing tank, coordinates were fixed with the glider model. The x-axis direction was aligned with the towing direction of the carriage. The towing carriage has a six-component force measuring mechanism to calculate the forces and moments acting on the glider model. Two force transducers were fixed along the x-axis direction, one was fixed along the y-axis, and three transducers were loaded in the vertical direction along the z-axis.

The tests consisted of the following configuration:

(1) Resistance test by towing the glider through the water body at variable (0.3, 0.5, 0.7 and 1 m/s) speeds, while being aligned to the direction of tow at zero drift angles.
(2) Horizontal static drift test with drift angles 6, 12, and 18 degrees. All runs were completed with speeds of 0.3, 0.5 and 0.7 m/s.

CFD method

Computational fluid dynamic (CFD) simulation was employed to investigate the hydrodynamic performance of the underwater glider. In this work, FLUENT version 16.1 was used for CFD simulation. This simulation solved the incompressible fluid flow field and pressure force around the glider hull based on the Reynolds Averaged Navier Stokes (RANS) equations[13].

The k-ξ model was selected as the turbulence model due to its robustness and wide application range[14]. The equations of the model are a modified form of RANS equations and are particularly applicable to slow-moving objects in a fluid stream such as a AUG moving in sea water[15]. The model equation is given in equations 9-11.

$$\rho\frac{\partial k}{\partial t}+\rho\frac{\partial\left(kU_j\right)}{\partial x_j}=-\rho\overline{u_i'u_j'}\frac{\partial U_i}{\partial x_j}-\rho\varepsilon+\frac{\partial}{\partial x_j}\left(\frac{\mu_t}{\sigma_k}+\mu\right)\frac{\partial k}{\partial x_j} \quad \ldots (9)$$

$$\rho\frac{\partial \varepsilon}{\partial t}+\rho\frac{\partial\left(\varepsilon U_j\right)}{\partial x_j}=-C_{\varepsilon 1}\frac{\varepsilon}{k}\rho\overline{u_i'u_j'}\frac{\partial U_i}{\partial x_j}-C_{\varepsilon 2}\rho\frac{\varepsilon^2}{k}+\frac{\partial}{\partial x_j}\left[\left(\frac{\mu_t}{\sigma_\varepsilon}+\mu\right)\frac{\partial \varepsilon}{\partial x_j}\right] \quad \ldots (10)$$

The intensity of turbulence viscosity can be calculated as:

$$\mu_t=\rho C_\mu k^{1/2} \quad \ldots (11)$$

Where the constant values in k-ξ turbulence model are:

$$C_{\varepsilon 1}=0.09,\quad C_{\varepsilon 2}=1.44,\quad \sigma_k=1.0,\quad \sigma_\varepsilon=1.30$$

Results and Discussion

Computational domain and boundary conditions

In this study, the fluid domain consists of the glider body, flow velocity inlet, pressure outlet, ceiling and bottom wall, and two side walls. A domain independence test analysis was conducted with different inlet, outlet and side wall positions with fine mesh using RNG k-ξ model at zero drift angle and Fr number of 0.33. The results of domain independency are summarized in Table which shows that the best domain size is $1.5L_{inlet}$ x$3.5L_{outlet}$x$9D_{side\text{-}wall}$. Figure 8 shows that the location of glider body was 1.5 times L_{glider} from flow inlet and 3.5 times L_{glider} from outlet boundary. Ceiling, bottom and side walls were defined as free slip wall boundary 9 times D_{glider} away from the no slip glider boundary to avoid the obstruction in the flow.

Grid independence analysis

The reliability of measurements is directly affected by the grid size and number of elements. Ideally for grid independency, three to four different grid sizes should be examined. In this study, different sizes of the grid were generated for

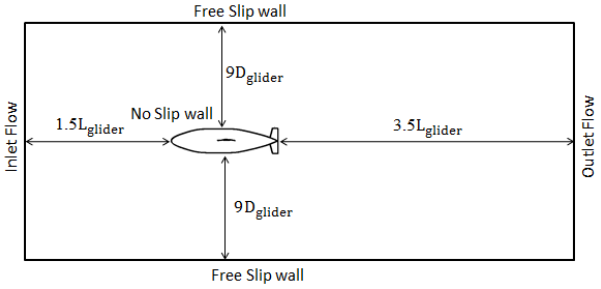

Fig. 8 — Fluid domain for CFD simulation

Table 2 — Fluid domain selection for CFD simulation

Domain Size	Drag Coefficient (CFD)	Experimental Values	Error (%)
$1.5L_{inlet}$ x$3.5L_{outlet}$x$6D_{side\text{-}wall}$	0.513387	0.563013	8.81
2 L_{inlet} x$4.5L_{outlet}$x9 D $_{side\text{-}wall}$	0.506191	0.563013	10.09
1.5 L_{inlet} x$3.5L_{outlet}$x9 D $_{side\text{-}wall}$	0.525011	0.563013	6.75
2 L_{inlet} x$4.5L_{outlet}$x6 D $_{side\text{-}wall}$	0.506191	0.563013	10.09
1.5 L_{inlet} x$4L_{outlet}$x6 D $_{side\text{-}wall}$	0.513305	0.563013	8.83
1.5 L_{inlet} x$4L_{outlet}$x9 D $_{side\text{-}wall}$	0.51074	0.563013	9.28

grid independency study because of limitation of computational time limitation and costs to simulate the 3D fluid domain with the glider. The grid independency results of drag and lift coefficients are shown in Figure 9 and 10. The mesh size for all simulations was 4×10^6 to 4.5×10^6. The suitable value of Y^+ for turbulence flow was fixed between 10 and 30 for standard wall function[16].

Influence of struts on resistance

The aero-foils were evaluated separately (without glider) to determine the influence of hydrodynamic forces on the total measurements, as shown in Figure 11.

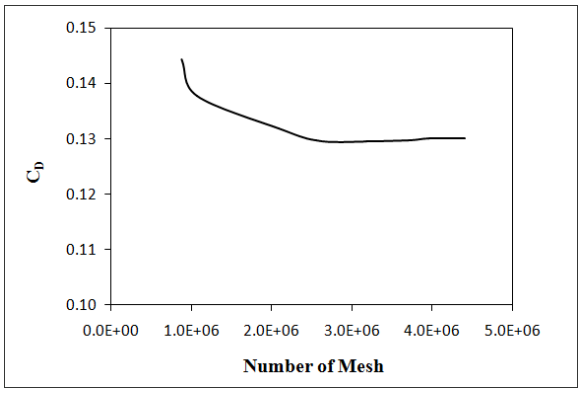

Fig. 9 — Drag coefficient grid independency numerical simulation

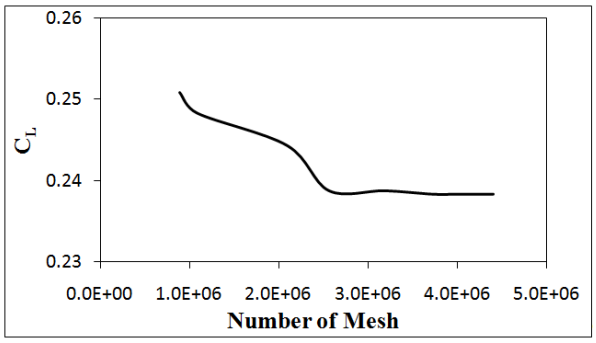

Fig. 10 — Lift coefficient grid independency numerical simulation

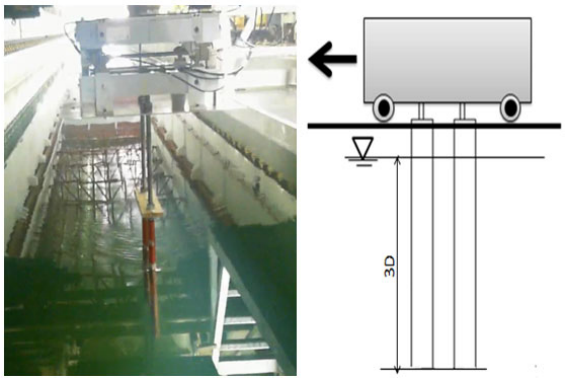

Fig. 11 — Experimental (left) and schematic (right) diagram of struts test

Table shows the variation in resistance force calculation with aero-foil struts. The results show that the resistance force increases with the velocity, because the resistance force is directly proportional to the velocity in laminar region and velocity square in the turbulence region[17]. It was observed, that the resistance was higher at higher Fr number because of vortices or turbulence across the struts, which was subtracted from the total resistance of the glider with struts.

Resistance characteristics

The measured total resistance force (RT) and its relationship with Froude numbers (Fr) at different drift angles are shown in Figure 12. The results show that the resistance value increases 77%, 77%, 85%

Table 3 — Percentage increment of resistance force with struts

Fr	Resistance force with struts	Resistance force of struts	%age increment of resistance due to struts
0.33	0.622765	0.059752	9.59
0.55	1.76437	0.449154	25.45
0.77	3.653227	1.182052	32.34
1.10	8.244253	2.938618	35.64

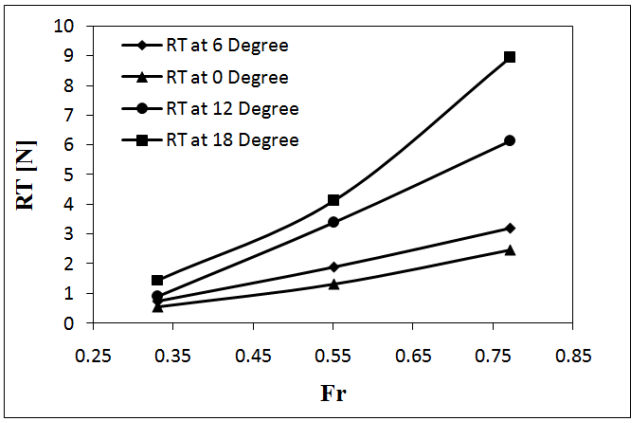

Fig. 12 — Experimental resistance force at various drift angle versus Froude number

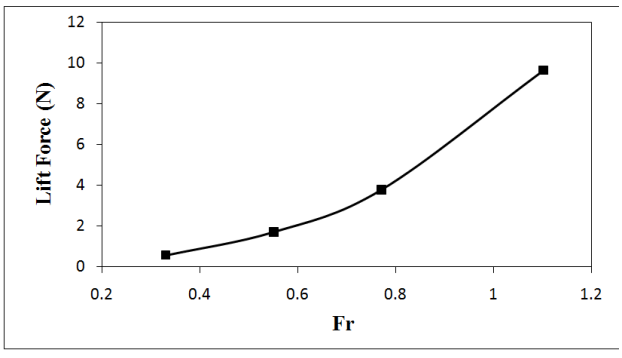

Fig. 13 — Experimental lift force verses Froude number at zero degree drift angle

and 83% for drift angle (β = 0°, 6°, 12° and 18°) in the range of Fr=0.33 to 0.77, respectively. Moreover, the overall resistance value increased by 61%, 68% and 72% with the increment of drift angle 6°, 12° and 18°, respectively. This is attributed to increase in speed and pressure around the glider hull, causing the boundary layer to move closer to the hull body, hence resulting in increased friction and viscosity. Moreover, the increase in blockage area by the drift angles also contributed significantly to the increase in resistance force.

Figure 13 illustrates the lift force deviation with respect to the Froude number (Fr) at zero drift angles. Lift force increased from 120% to 198% at zero degrees for Froude number (Fr=0.33 to 0.77). The key source to generate high lift force is flow separation, because high pressure forces act on the front side (opposite to fluid direction) of glider and negative pressure was generated back side of the glider. Hence, this negative pressure leads to huge amount of lift force.

Comparison of experimental and numerical results

Resistance (RT) force: The experimental and numerical values for resistance force on the glider model are shown in Figure 14 and Table .

Generally, the numerical simulation results are in good agreement with experimental results, with a maximum error of 6.9%. The difference between the experimental and numerical calculations can be attributed to test conditions. In the experiments, the glider model was towed with the help of a carriage while in simulation the flow was created around the glider model. The discrepancies may have occurred due to the variation of carriage speed or flow vortices around the glider. Similarly, some discrepancies may be due to the selection of flow model or number of inflation layers and selection of fluid domain in the numerical simulation. Figure 15 presents the total resistance force (RT) and its relationship with Froude numbers (Fr) at different drift angles.

Lift force (F_L): The normal component of the resultant force when the glider is moving through the fluid is called lift force. Normally, lift force is a function of fluid density, velocity of fluid and shape of glider. Figure 16 shows that the numerically predicted trend of lift force is similar to that of the experimental results. It can be seen that the lift force increases with the increment of the Froude number (Fr) at zero drift angles.

Table 4 — Comparison of resistance force at zero drift angles

Fr	CFD Results	Experiment Results	Error (%)
0.33	0.577494	0.563013	2.50
0.55	1.393193	1.315216	5.59
0.77	2.617866	2.471175	5.60
1.10	4.962295	5.305635	6.91

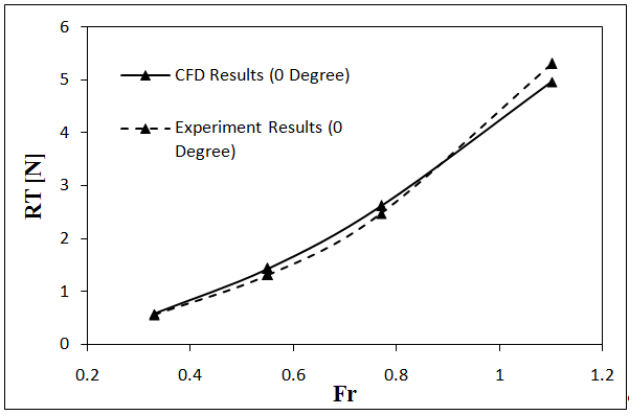

Fig. 14 — Variation in resistance of glider versus Froude number

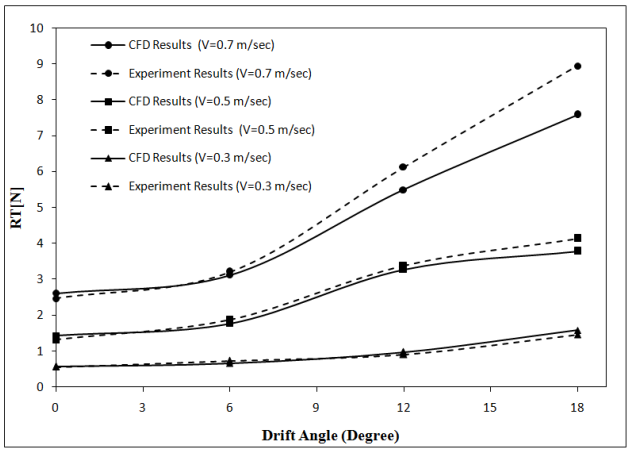

Fig. 15 — Variation in resistance of glider versus Froude number with certain drift angle

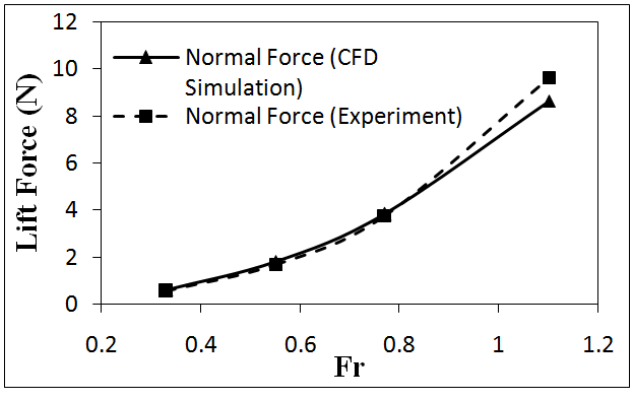

Fig. 16 — Variation of lift force vs Froude number at zero degree of drift angle

Conclusion

The lift force (normal force) and resistance (RT) of a newly developed underwater glider are investigated experimentally (towing tank test) and numerically under different operational conditions such as speed and drift angle. The results of this study show that the increment of lift forces is higher compared to the resistance force with increasing drift angle and speed.

These results are helpful in designing gliders with better manoeuvrability and control surface for an underwater glider with similar shape, wings and operational conditions. A comparison study of numerical simulation and experimental results shows a good agreement. Hence, the numerical simulation of hydrodynamic characteristics on glider with wings resembles with glider model.

Acknowledgement

Authors are thankful to Universiti Teknologi PETRONAS for providing the resources required for this work.

References

1 (a) Graver, J. G.; Bachmayer, R.; Leonard, N. E.; Fratantoni, D. M. In *Underwater glider model parameter identification*, Proceedings of the 13th International Symposium on Unmanned Untethered Submersible Technology, 2003; (b) Bender, A.; Steinberg, D. M.; Friedman, A. L.; Williams, S. B. In *Analysis of an autonomous underwater glider*, Proceedings of the Australasian Conference on Robotics and Automation, 2008; pp 1-10.

2 Stevenson, P.; Furlong, M.; Dormer, D. In *AUV shapes-combining the practical and hydrodynamic considerations*, OCEANS 2007-Europe, IEEE: 2007; pp 1-6.

3 Webb, D. C.; Simonetti, P. J.; Jones, C. P., SLOCUM: An underwater glider propelled by environmental energy. *Oceanic Engineering, IEEE Journal of* 2001, *26* (4), 447-452.

4 Sherman, J.; Davis, R.; Owens, W.; Valdes, J., The autonomous underwater glider" Spray". *Oceanic Engineering, IEEE Journal of* 2001, *26* (4), 437-446.

5 Eriksen, C. C.; Osse, T. J.; Light, R. D.; Wen, T.; Lehman, T. W.; Sabin, P. L.; Ballard, J. W.; Chiodi, A. M., Seaglider: A long-range autonomous underwater vehicle for oceanographic research. *Oceanic Engineering, IEEE Journal of* 2001, *26* (4), 424-436.

6 Moonesun, M.; Javadi, M.; Charmdooz, P.; Mikhailovich, K. U., Evaluation of submarine model test in towing tank and comparison with CFD and experimental formulas for fully submerged resistance. *Indian Journal of Geo-Marine Sciences* 2013, *42* (8), 1049-1056.

7 Bertram, V., *Practical ship hydrodynamics*. Elsevier: 2012.

8 Jackson, H. A.; Technology, M. I. o., *Submarine Design Notes*. Massachusetts Institute of Technology: 1982.

9 Azarsina, F.; Williams, C. D., Manoeuvring simulation of the MUN Explorer AUV based on the empirical hydrodynamics of axi-symmetric bare hulls. *Applied Ocean Research* 2010, *32* (4), 443-453.

10 Molland, A. F.; Turnock, S. R.; Hudson, D. A., *Ship resistance and propulsion: practical estimation of propulsive power*. Cambridge university press: 2011.

11 Committee, I. S. In *Final report and recommendation to the 23rd ITTC [C]*, The 23rd proceedings of International Towing Tank conference. Venice, Italy, 2002; pp 1-5.

12 Muhammad Yasar; Javaid ; Mark; Ovinis; Nagarajan; Thirumalaiswamy; Fakhruldin B M; Hashim; Adi; Maimun; Barkat Ullah, Dynamic Motion Analysis of a Newly Developed Autonomous Underwater Glider with Rectangular and Tapered Wing. *Indian Journal of Geo-Marine Sciences* 2015, *Vol. 44(12)* (December 2015), 1928-1936.

13 (a) Ferziger, J. H.; Peric, M., *Computational methods for fluid dynamics*. Springer Science & Business Media: 2012; (b) Roddy, R. F. *Investigation of the stability and control characteristics of several configurations of the DARPA SUBOFF model (DTRC Model 5470) from captive-model experiments*; DTIC Document: 1990.

14 Phillips, A. B. Simulations of a self propelled autonomous underwater vehicle. University of Southampton, 2010.

15 (a) Wang, Y.; Gao, T.; Pang, Y.; Tang, Y., Investigation and optimization of appendage influence on the hydrodynamic performance of AUVs. *Journal of Marine Science and Technology* 2019, *24* (1), 297-305; (b) Candries, M.; Anderson, C.; Atlar, M. In *Foul release systems and drag*, Proceedings of the PCE 2001 Conference, Antwerp, 2001; pp 273-286.

16 Javaid, M. Y.; Ovinis, M.; Hashim, F. B. M.; Maimun, A.; Ahmed, Y. M.; Ullah, B., Effect of wing form on the hydrodynamic characteristics and dynamic stability of an underwater glider. *International Journal of Naval Architecture and Ocean Engineering* 2017, *9* (4), 382-389.

17 (a) Mitra, A.; Panda, J. P.; Warrior, H. V., The effects of free stream turbulence on the hydrodynamic characteristics of an AUV hull form. *Ocean Engineering* 2019, *174*, 148-158; (b) Falkovich, G., *Fluid mechanics: A short course for physicists*. Cambridge University Press: 2011.